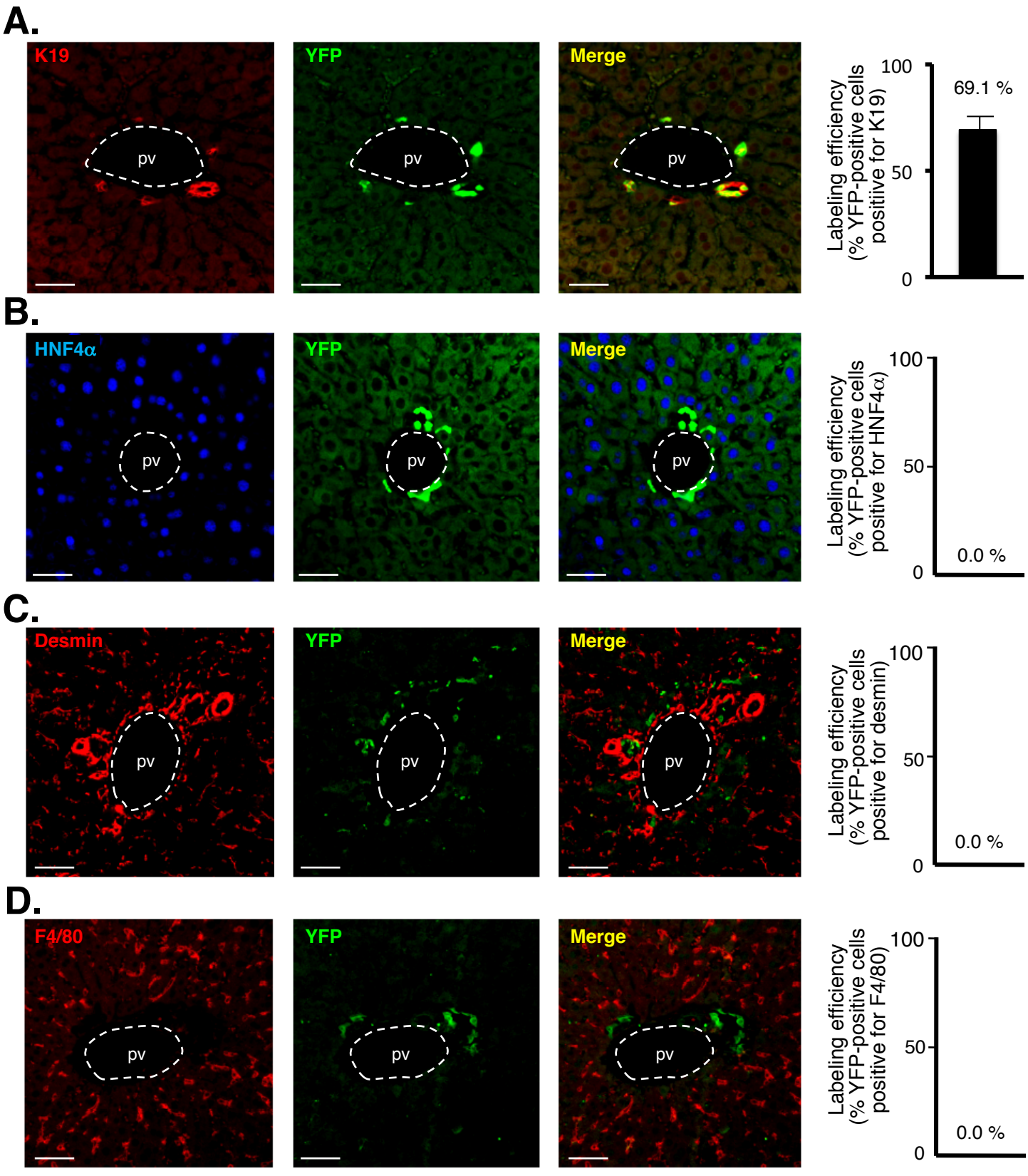

Supplementary Figure 1. OPN-CreERT2 efficiently and selectively labels the liver progenitor cell/ biliary compartment. OPN-CreERT2 mice were subjected to 2 consecutive tamoxifen injections and labeling efficiency was quantified prior inducing tumor formation. **A.** Liver sections were stained for YFP and K19. Co-localization was determined by confocal microscopy and quantified. **B-D.** Liver sections were stained for YFP and HNF4α (B), desmin (C) or F4/80 (D). Co-localization was determined by confocal microscopy and quantified (quantification in 15 mice, 800-1000 K19+ cells/mouse). Scale Bar 40 μm; p.v., portal vein

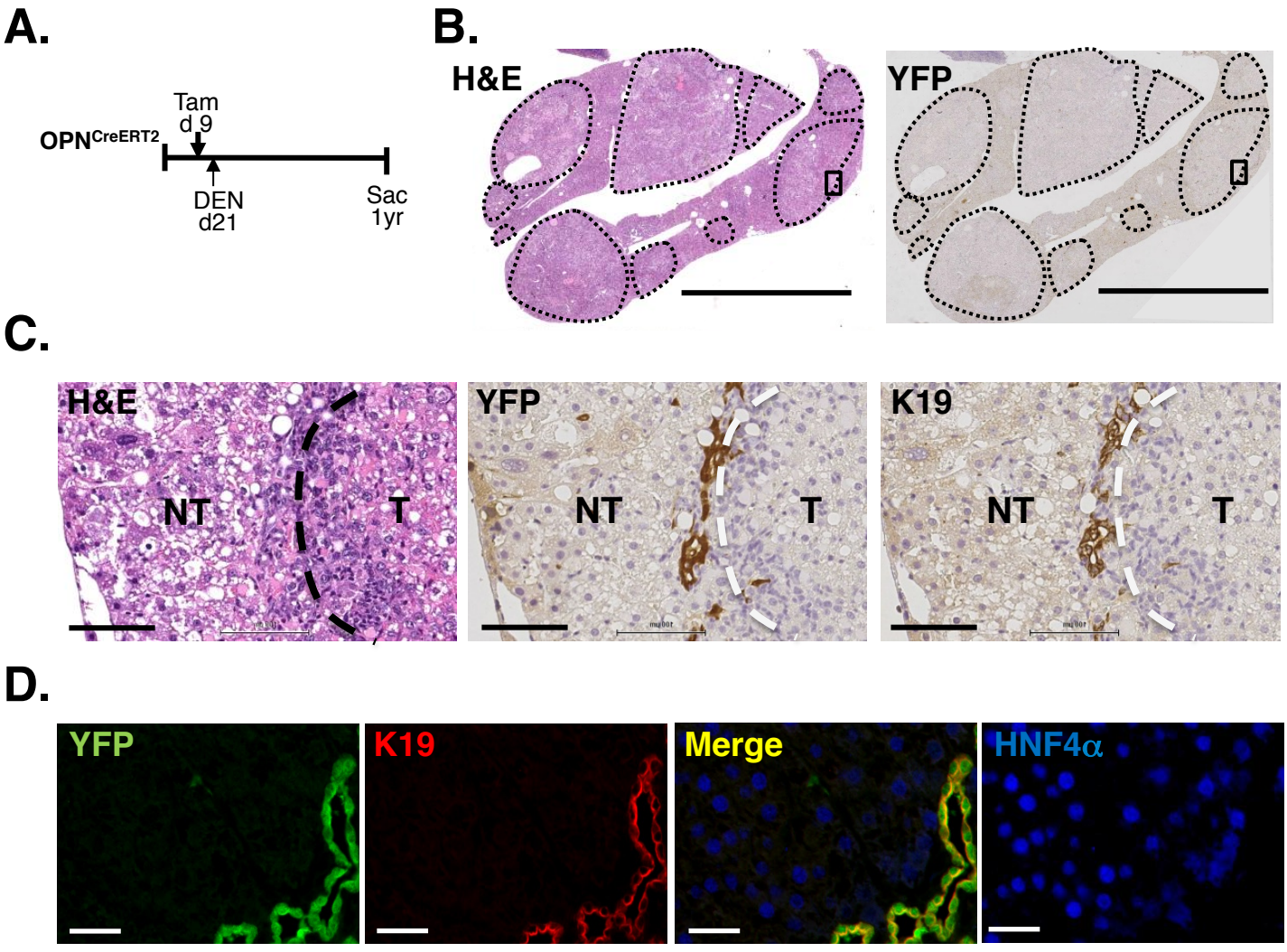

Supplementary Figure 2. HCC does not derive from OPN-CreERT2 labeled liver progenitor cells in mice with single DEN injection. **A.** HCC were induced by a single injection of DEN to OPN-CreERT2 mice at d15. **B.** Slide of a representative liver stained with H&E and YFP showing multiple tumors all devoid of YFP expression. **C**. At microscopic examination, YFP expression is restricted to the peritumoral ductular reaction and bile ducts. **D.** Immunofluorescence confirmed colocalization of YFP with K19-positive DR. Scale bars B: 1 cm; C: 100 μm; D: 50 μm.

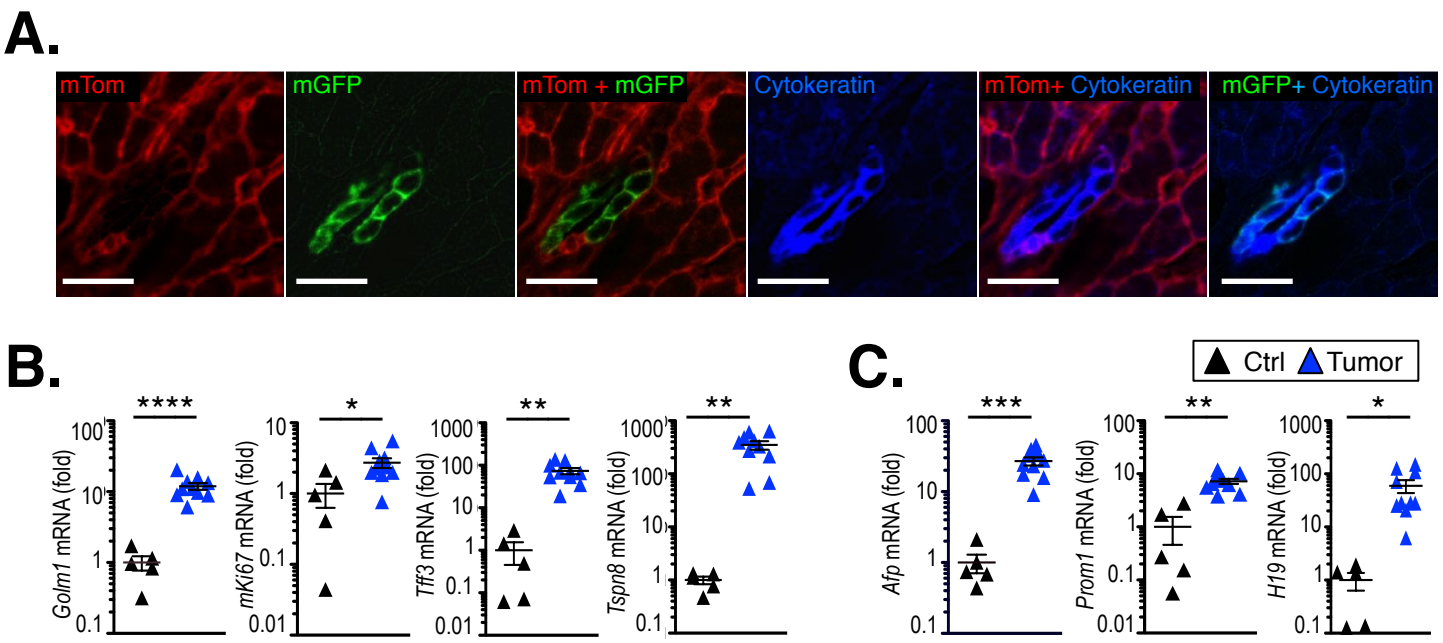

Supplementary Figure 3. LPC/biliary compartment tracing by K19-CreERT in the DEN+CCl_4 hepatocarcinogenesis model. mTom-mGFP Cre reporter mice (n=5) were treated with tamoxifen followed by single injection with DEN and 20 CCl_4 injections for HCC induction. **A.** Immunofluorescent staining and confocal microscopy demonstrate specific labeling of the LPC/biliary compartment, as demonstrated by co-localization of mGFP and K19. **B-C.** HCC markers (B) and progenitor/hepatoblast markers (C) were determined by qPCR (n=5 Ctrl, n=10 Tumor). Scale bars: 50 μm. *p<0.05; ** p<0.01; ***p<0.001. Statistical significance was determined by two-sided T-test.

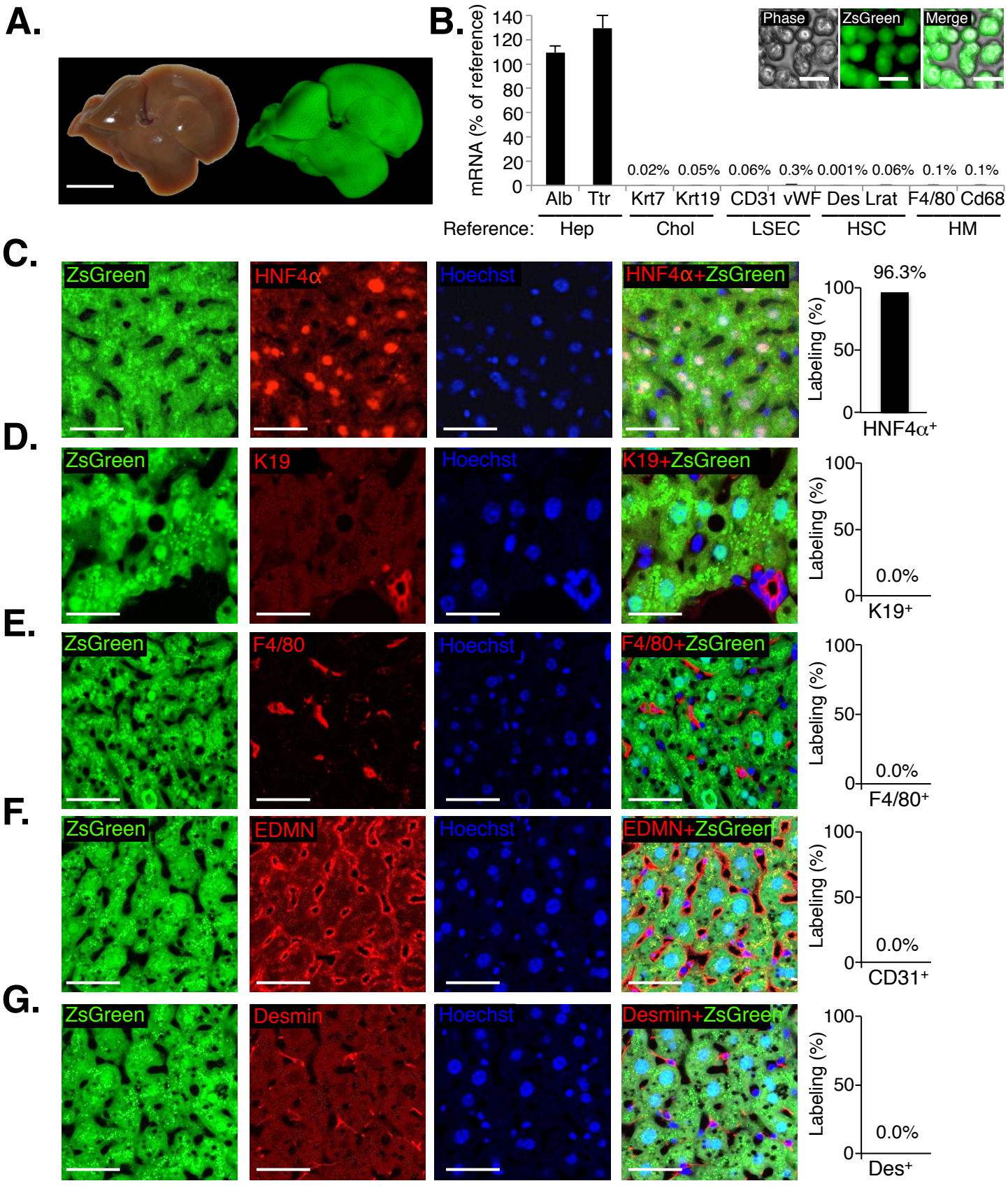

Supplementary Figure 4. AAV8-TBG-CRE labels hepatocytes but not bile ducts, macrophages, endothelial cells or hepatic stellate cells. A-B. ZsGreen mice were injected with AAV8-TBG-Cre. One week after injection, green-fluorescent cells were isolated from the liver and the expression of hepatocyte, cholangiocyte, LSEC, HSC and HM markers was compared between the green fluorescent cells and pure populations of hepatocytes, cholangiocytes, LSEC, HSC and HM (n=2). **C-F.** Liver sections were stained for HNF4α, K19, F4/80, endomucin (EDMN) and desmin. Co-localization of each marker with ZsGreen was determined by confocal microscopy and quantified (n=2). Scale bars: A: 1 cm, C, E-G: 100 μm, D: 50 μm

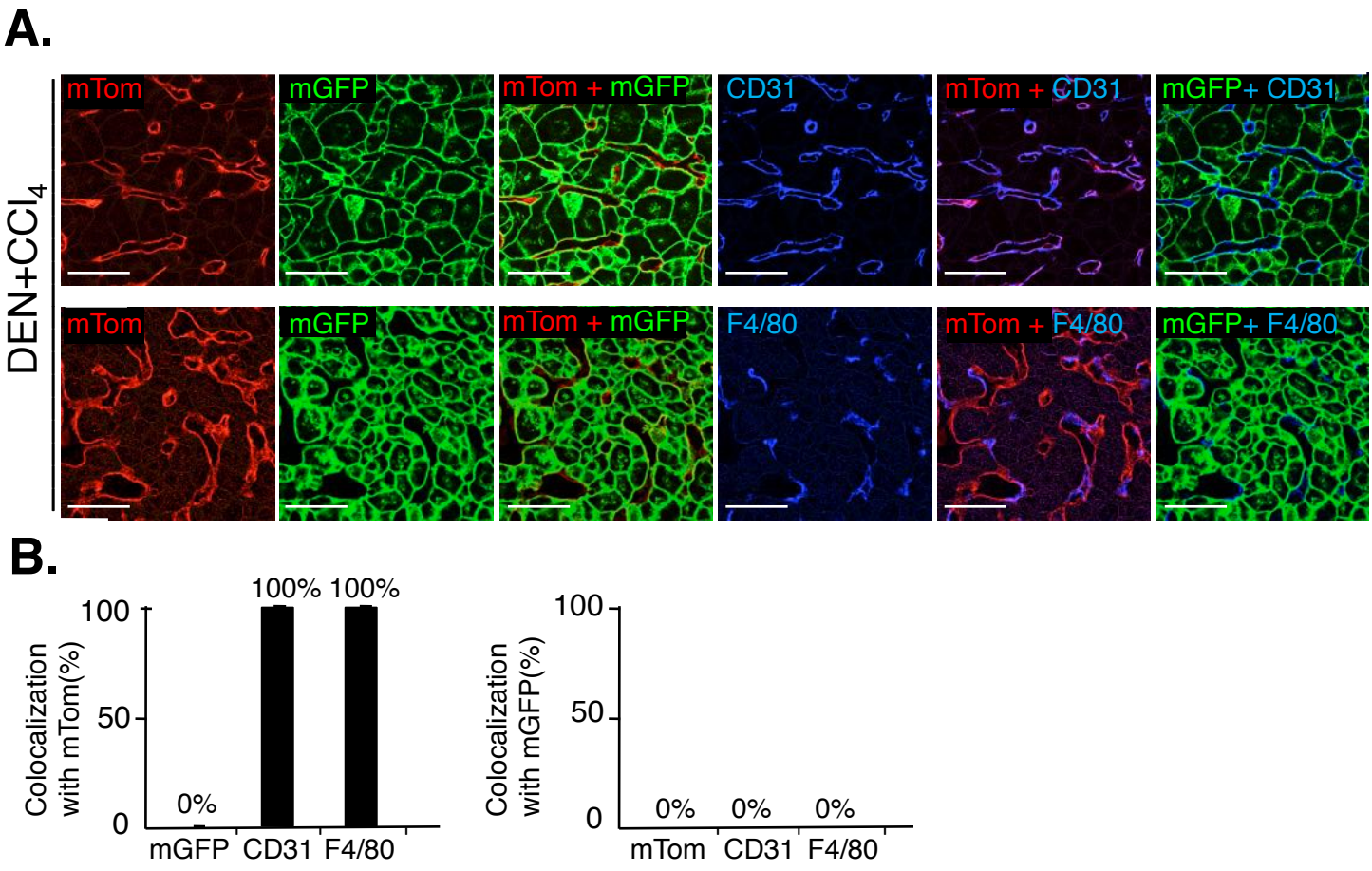

Supplementary Figure 5. mTom-positive cells within DEN+CCl_4-induced HCCs are CD31-positive endothelia and F4/80-positive macrophages. A. HCCs from AAV8-TBG-Cre-injected DEN+CCl_4-treated mTom-mGFP mice were stained for CD31 and F4/80, demonstrating co-localization of endothelial cell marker CD31, macrophage marker F4/80, with mTom, but no colocalization with mGFP**. B.** Quantification of colocalization of mGFP-positive cells with mTom, CD31 and F4/80 (n=10). Scale bars: 50 μm

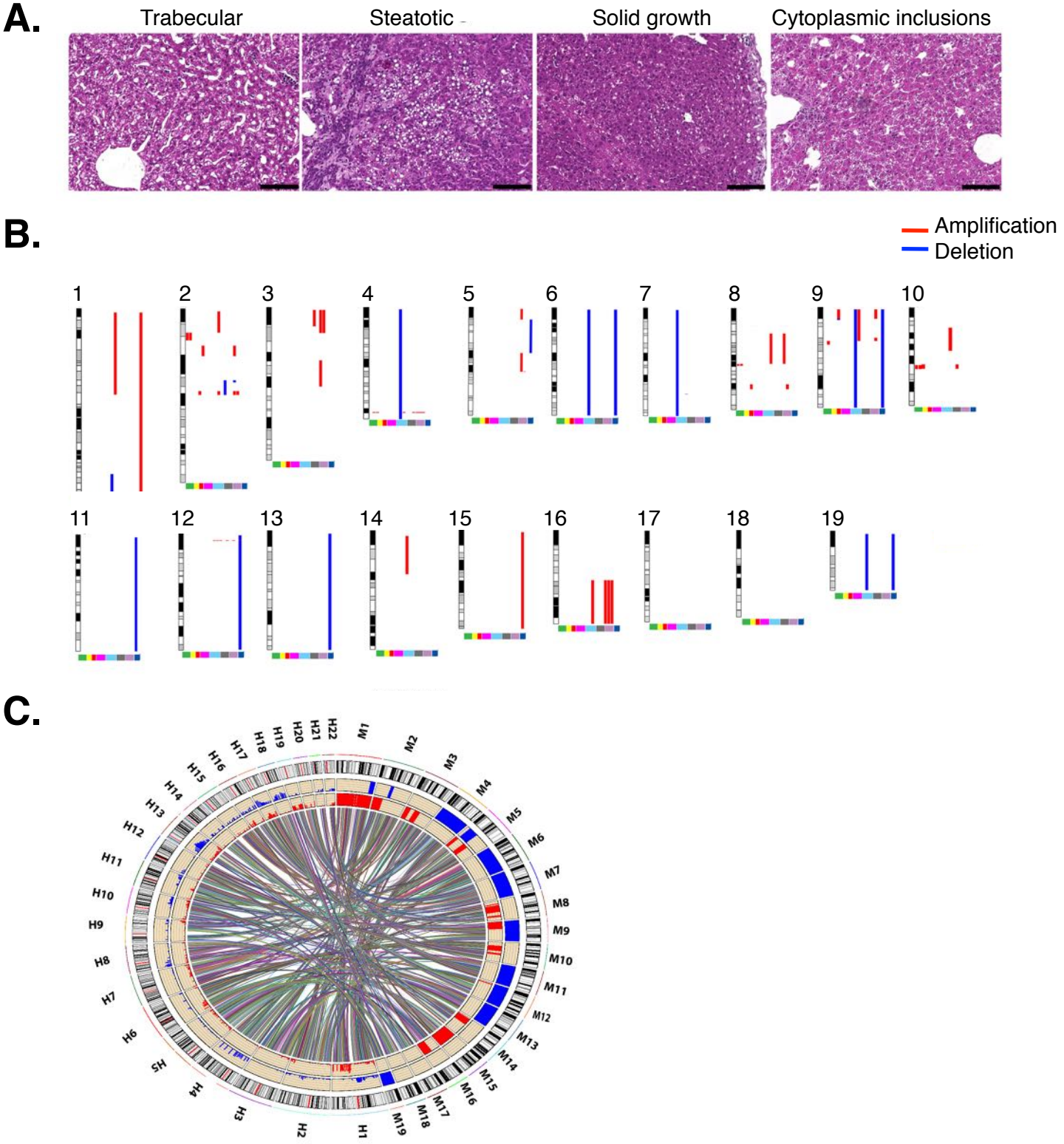

Supplementary Fig. 6. Characterization of DEN plus CCL_4-induced tumors. A. H&E staining reveals different growth patterns of tumors (n=10). **B.** Karyoplot of comparative genomic hybridization array from 19 tumors (from different 8 different mice). Long (q) arm is shown, dark band representing G-C rich domains, chromosomal deletions shown in red whereas amplifications are shown in blue. Each colored box represents one individual mouse. All mice analyzed show chromosomal aberrations, but there is no common pattern. Four tumors show deletions in chromosome 16. **C.** Synteny analysis comparing chromosomal aberrations of DEN+ CCL_4 induced and human cryptogenic HCCs. The plot reveals loci undergoing chromosomal losses (blue) or amplifications (red) found in the DEN + CCL_4 model are also found in human HCCs.

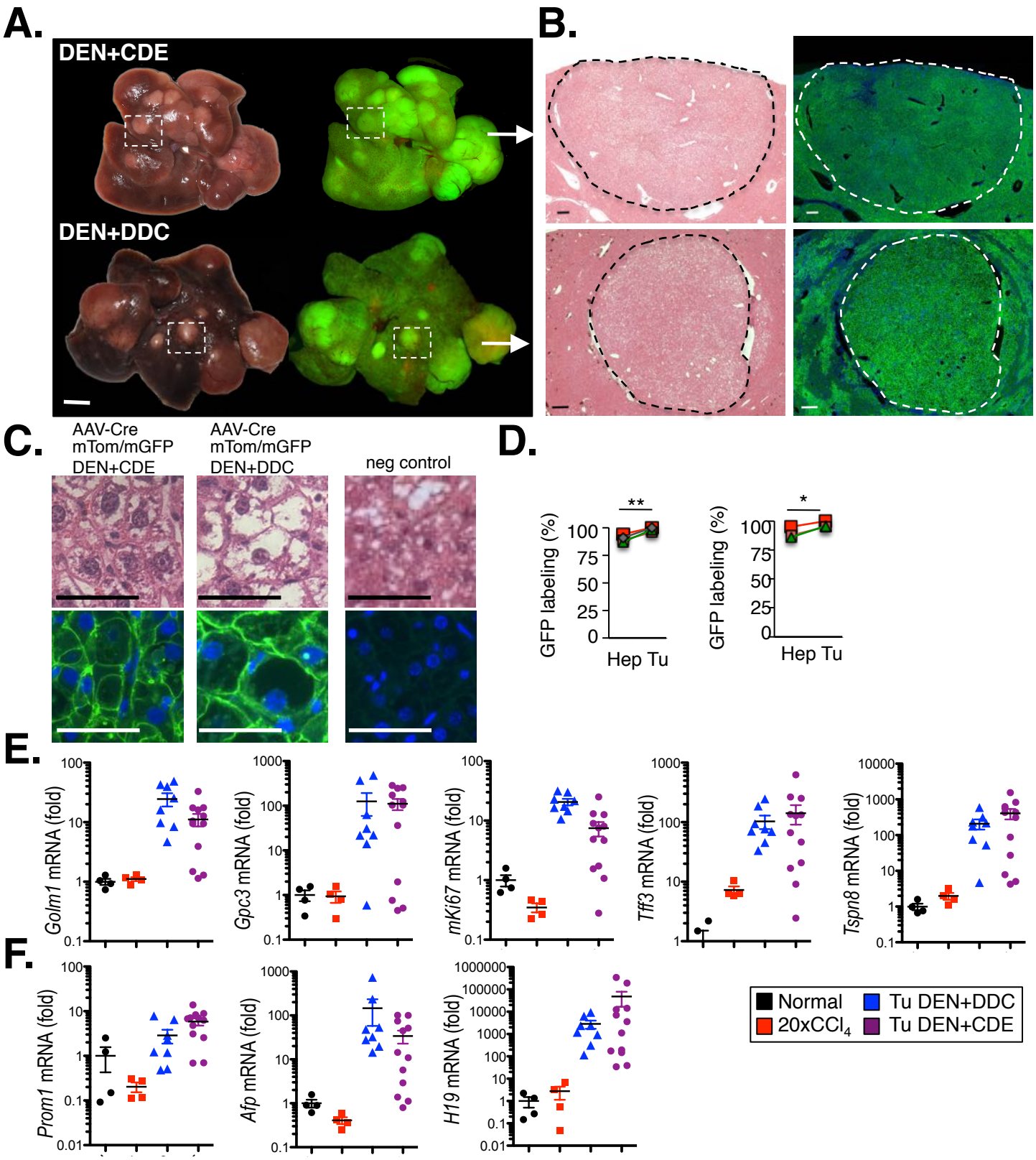

Supplementary Figure 7. HCCs are derived from hepatocytes even when hepatocarcinogenesis occurs in settings with abundant progenitors. mTom-mGFP Cre reporter mice were infected with AAV8-TBG-Cre to selectively label hepatocytes, followed by treatment with DEN and then either CDE (n=4) or DDC (n=3) diet for HCC induction**. A-D**. Representative photographs and fluorescent images of whole livers from DEN+CDE or DEN+DDC treated mice (A) and H&E- and GFP-stained liver sections at low (B) and high (C) magnification, including a mTom-mGFP-negative control. Quantification of GFP-labeled tumor and the corresponding percentage of mGFP-labeled hepatocytes (D, each color representing a single mouse). **E-F.** HCC (E) and progenitor markers (F) were determined by qPCR (n=4 normal, n=4 20xCCl$_4$, n=8 DEN+DDC tumors, n=12 DEN+CDE tumors). Scale bar A : 1 cm; B. 200 μm; C: 50 μm

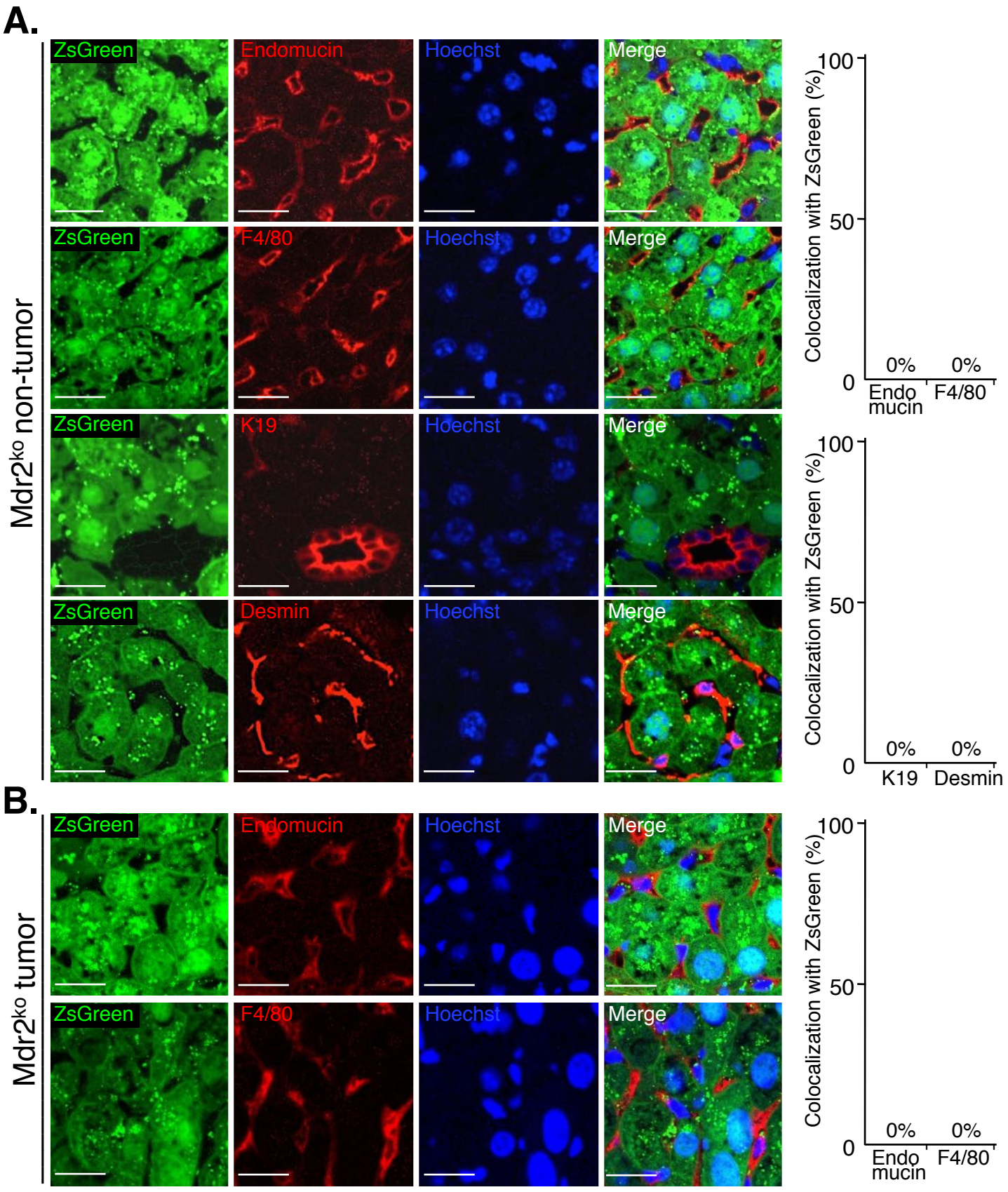

Supplementary Figure 8. ZsGreen-negative cells within HCCs from Mdr2^{ko} mice are CD31-positive endothelia and F4/80-positive macrophages. A. Non-tumor liver from AAV8-TBG-Cre-injected Mdr2^{ko} ZsGreen transgenic mice was stained for endomucin, F4/80, K19 and desmin, demonstrating absence of co-localization of these markers with ZsGreen **B.** HCCs from AAV8-TBG-Cre-injected Mdr2^{ko} ZsGreen transgenic mice were stained for endomucin and F4/80, demonstrating absence of co-localization of ZsGreen with endothelial cell and macrophage markers (n=2). Scale bars: 25 μm

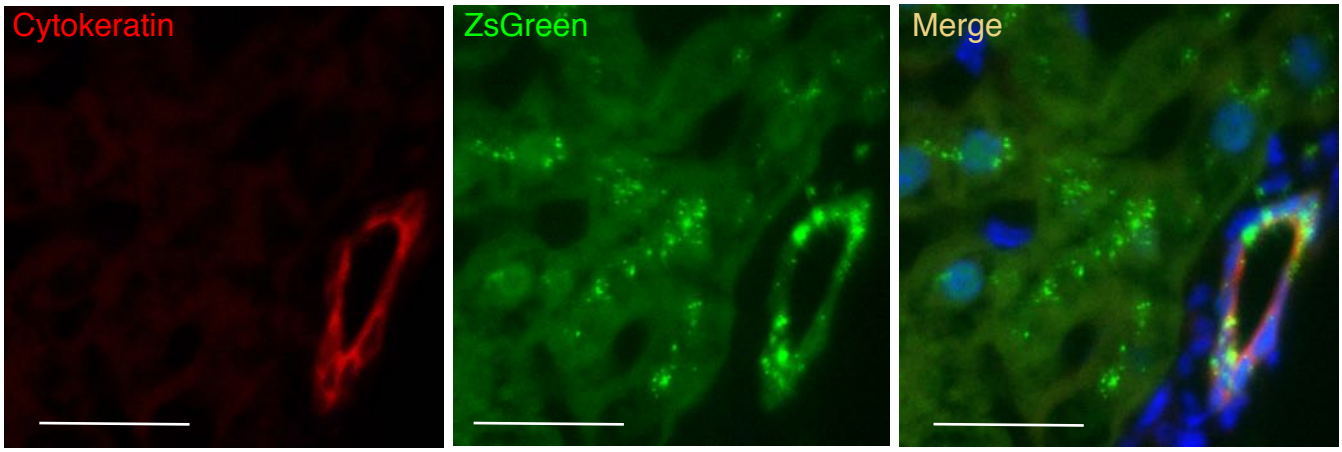

Supplementary Figure 9. Albumin-Cre deletes in the hepatocyte and biliary compartment. Confocal microscopy shows shows colocalization of pan-cytokeratin (marking bile ducts) and Cre reporter ZsGreen in Alb-Cre x ZsGreen mice (representative image from a total of 4 mice). Scale bars 50 μm

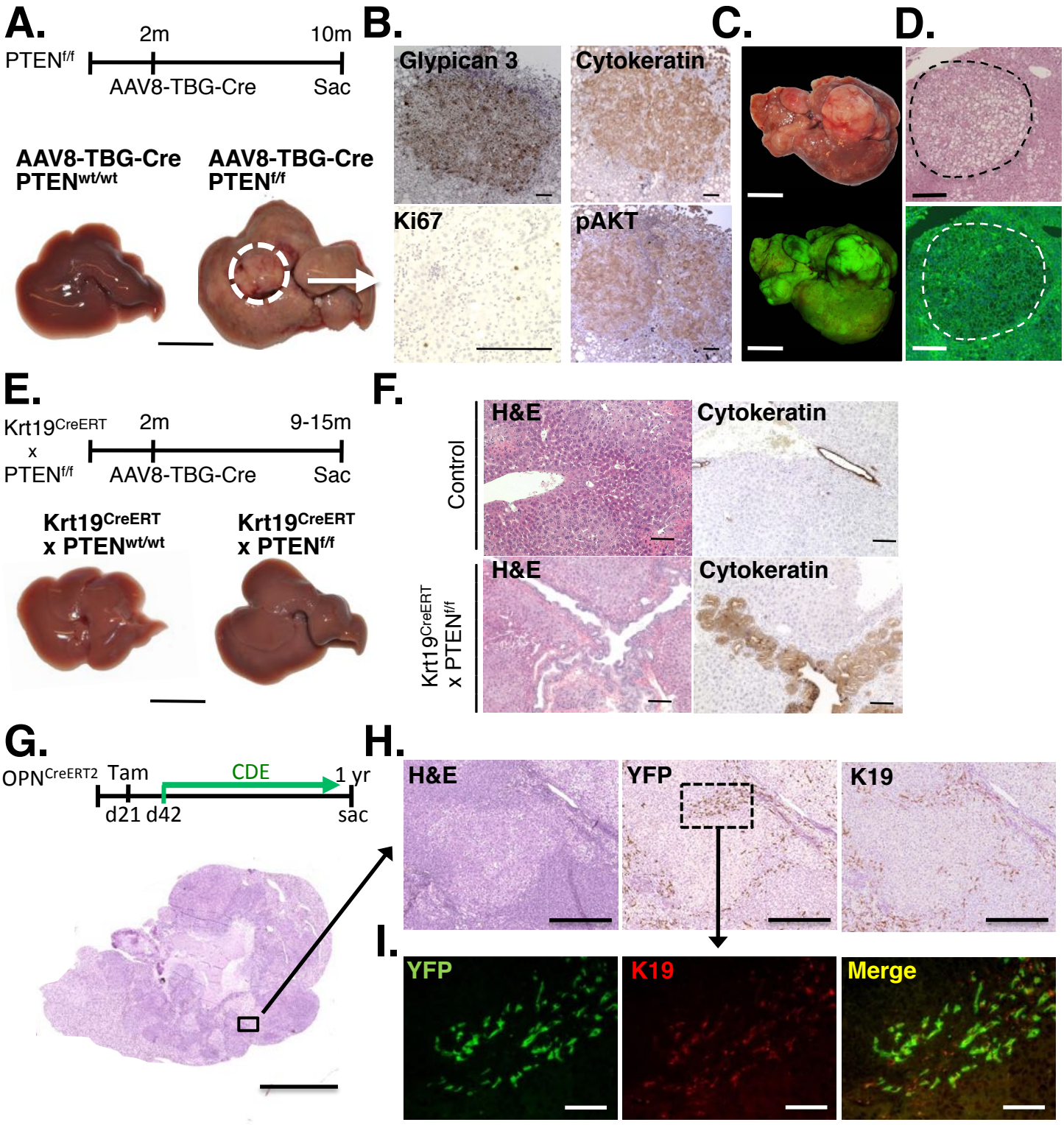

Supplementary Figure 10. HCCs derive from hepatocytes but not from liver progenitor cells in non-genotoxic murine hepatocarcinogenesis models. A-B. Hepatocyte-specific deletion of was achieved by infecting PTEN$^{wt/wt}$ (n=4) or PTEN$^{fl/fl}$ mice (n=8) with AAV8-TBG-Cre. After 10 months, macroscopic HCCs had developed in PTEN-deleted mice (A). HCC displayed loss of PTEN, increased expression of phosphorylated Akt (pAKT), positive glypican 3 and cytokeratin 19 staining (B). **C-D.** PTEN-deletion induced HCCs were hepatocyte-derived as shown by mGFP-mTom fluorescence. **E-F.** PTEN deletion in the progenitor/biliary compartment was achieved by tamoxifen-injection into Krt19CreERT x PTEN$^{fl/fl}$ mice (n=4) or PTEN$^{wt/wt}$ mice (n=4). No macroscopic tumors developed (D), but PTEN-deleted mice displayed expansion of the K19-positive cell compartment (E). **G-I**. Tamoxifen-injected OPN-CreERT2 mice were fed a CDE diet for 50 weeks to chronically stimulate LPC (H). All YFP-positive cells colocalized with K19-positive cells of the DR (I). Scale bars A and E: 1 cm; B: 250 µm; C: 1 cm. ; D,H: 200 µm; G 1cm; I: 100 µm.

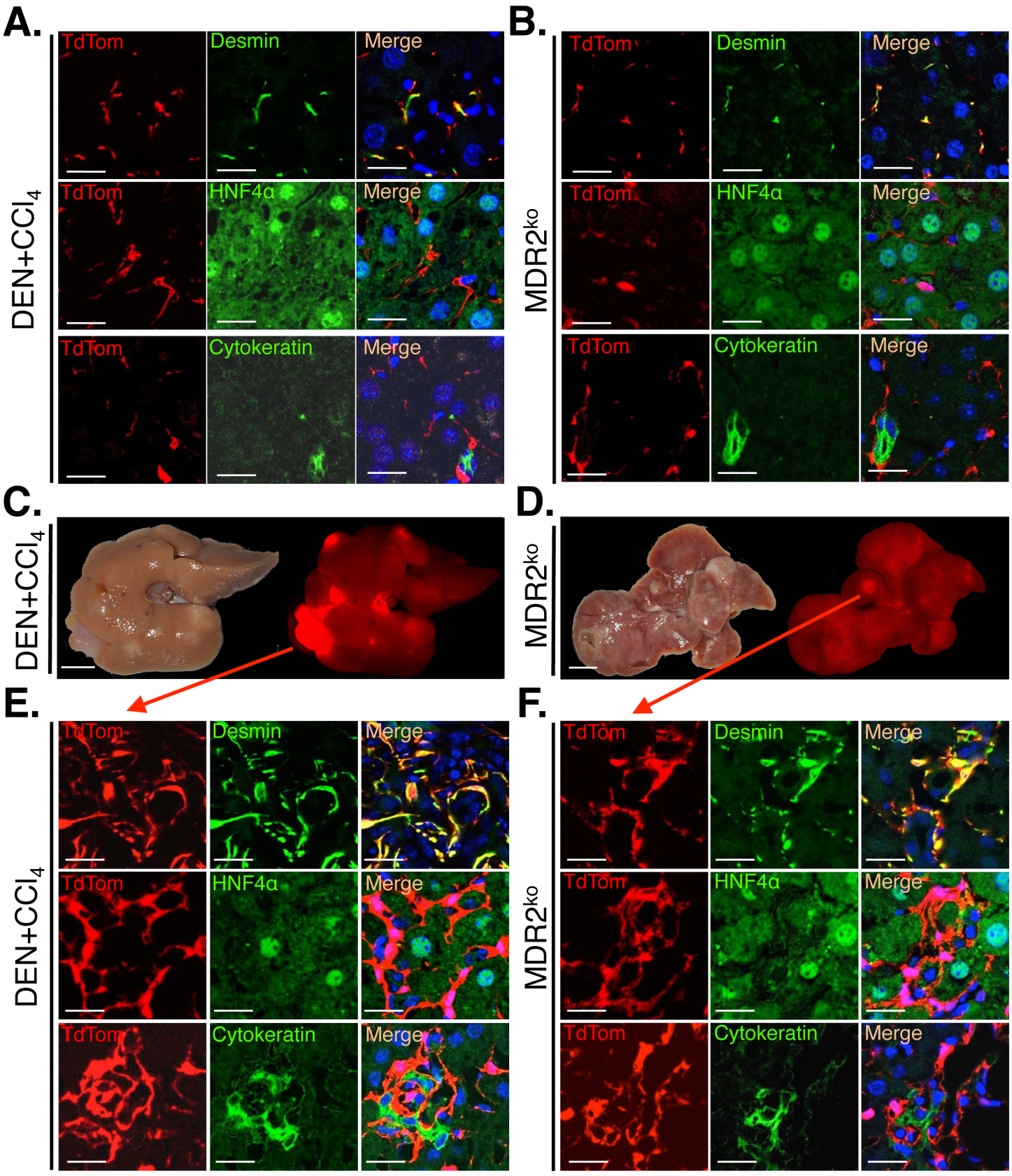

Supplementary Figure 11. LratCre-labeled cells within tumors are hepatic stellate cells. A-B. To determine the identy of LrateCre-labeled cells within DEN+CCl_4- (A) or $Mdr2^{ko}$-induced (B) tumors, we co-stained for desmin, HNF4α and cytokeratin (n=2-3 mice/group). Cells marked by Cre reporter TdTom always co-localized with HSC marker desmin, but never with HNF4α or cytokeratin. **C-F.** Some DEN+CCl_4- (C) or $Mdr2^{ko}$-induced (D) tumors from LratCre mice showed strong TdTom fluorescence. Costaining with desmin, HNF4α and cytokeratin in these tumors again revealed exclusive co-localization of TdTom with desmin but not with HNF4α or cytokeratin (n=2-3 mice/group). Scale bars A,B,E, and F: 50 μm; C and D: 500 mm.

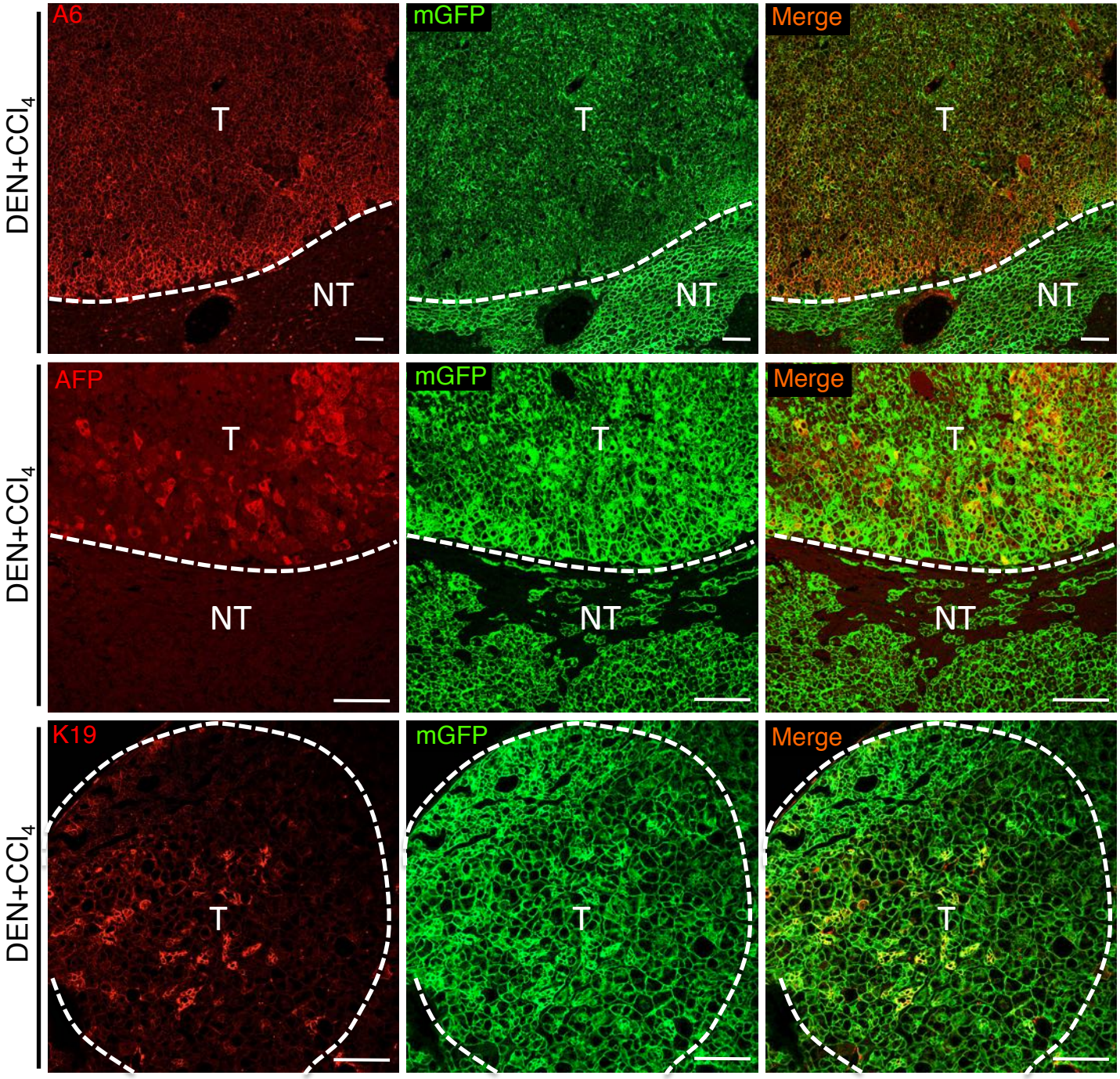

Supplementary Fig. 12. A6-, CK19- and AFP-positive liver progenitors within HCCs are derived from hepatocytes. Determination of the cellular origin of liver progenitor cells within HCCs, colocalization of progenitor markers AFP (A) A6 (B) and K19 (C) with mGFP was determined by confocal microcopy in tumor and non-tumor areas of mTom-mGFP mice whose hepatocytes had been labeled via AAV8-TBG-Cre and that were subsequently treated with DEN and CCl_4. Scale bars: 100 μm. T=tumor; NT=non-tumor

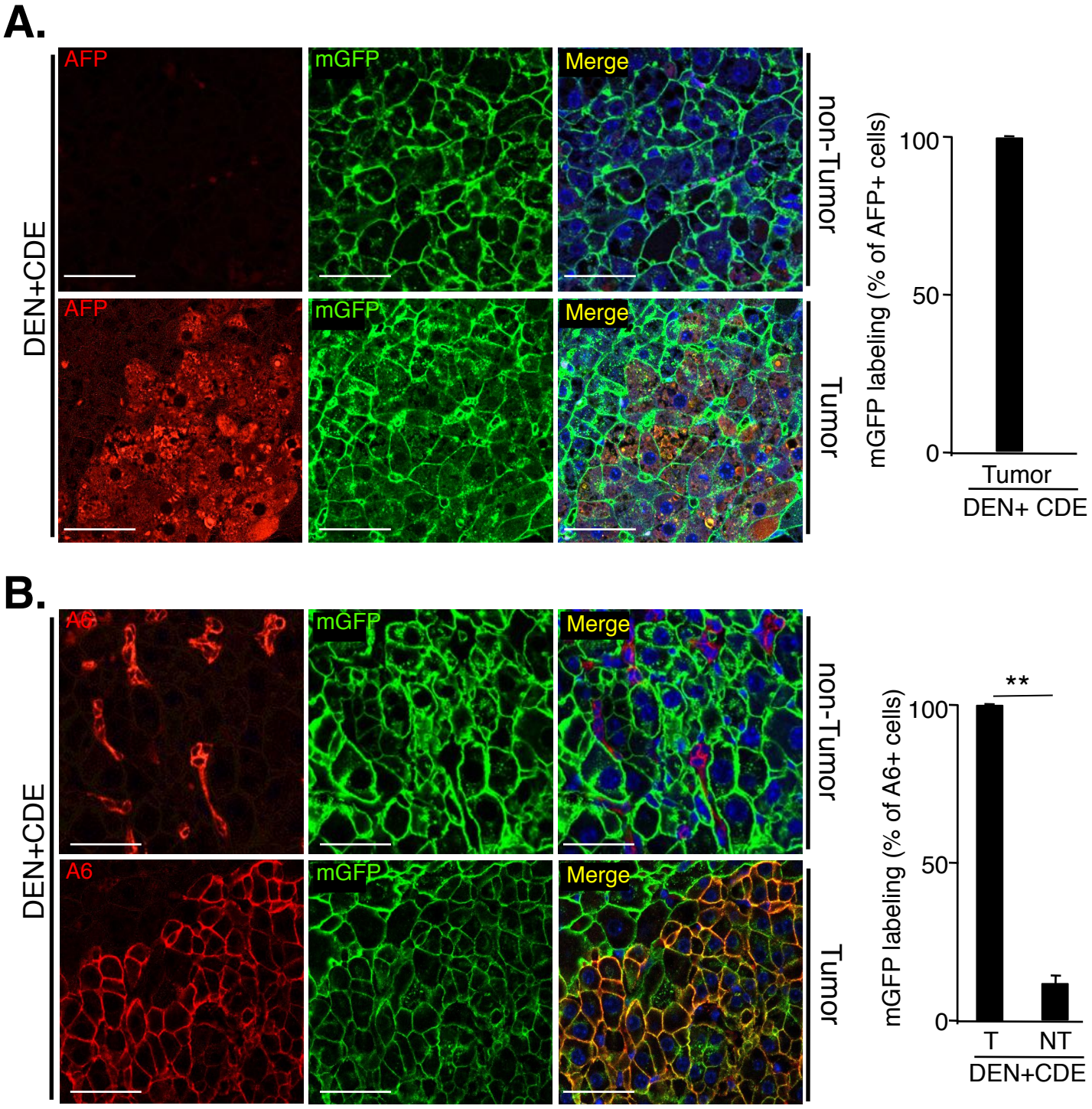

Supplementary Figure 13. A6- and AFP-positive liver progenitors within HCCs are derived from hepatocytes. A-B. Colocalization of progenitor markers AFP (A) and A6 (B) with mGFP was determined by confocal microcopy in tumor and non-tumor areas of mTom-mGFP mice whose hepatocytes had been labeled via AAV8-TBG-Cre and that were subsequently treated with DEN and CDE diet (n=3). Scale bars 50 µm. ** p<0.01. Statistical significance was determined by two-sided T test.

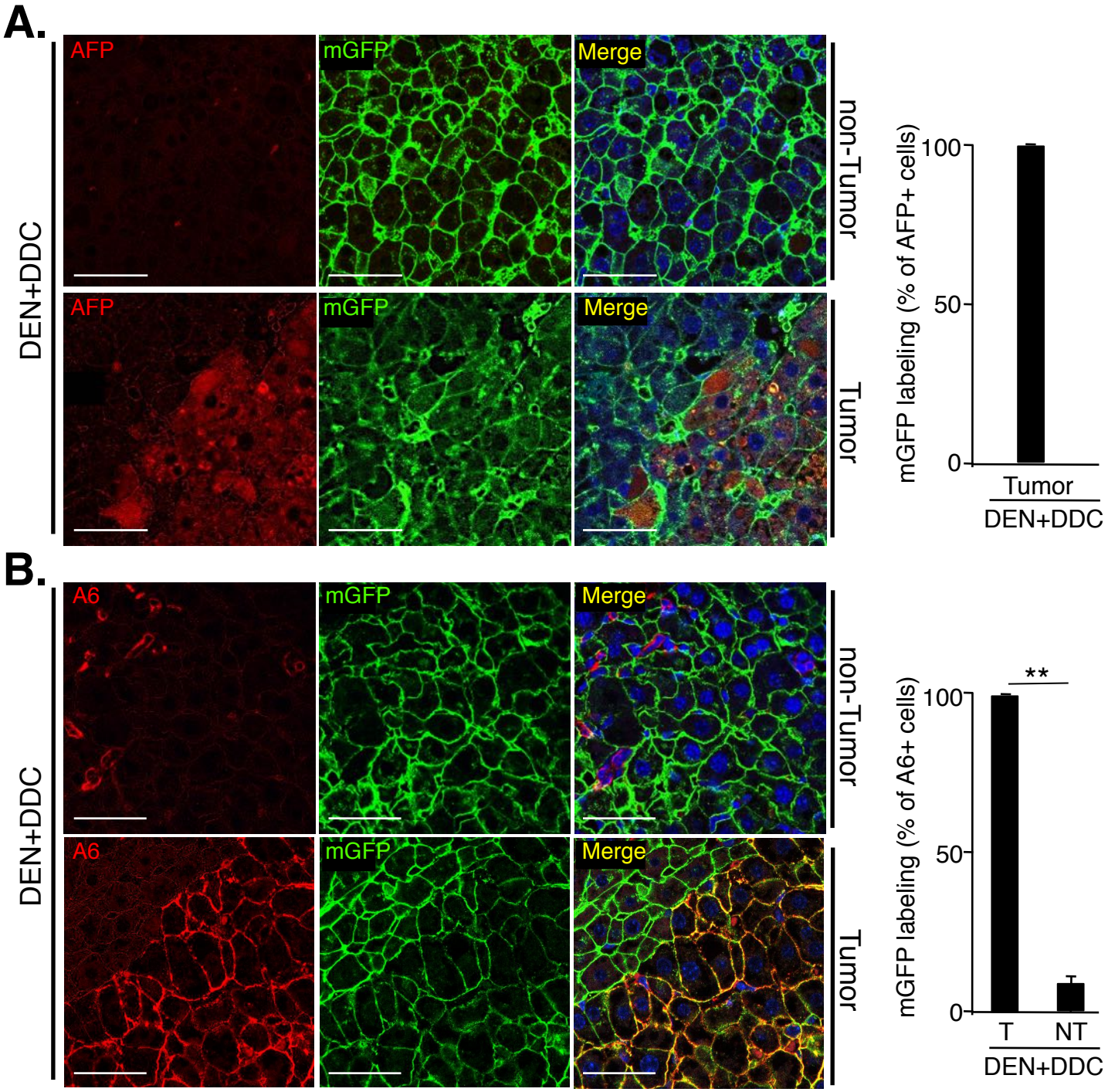

Supplementary Figure 14. A6- and AFP-positive liver progenitors within HCCs are derived from hepatocytes. A-B. Colocalization of progenitor markers AFP (A) and A6 (B) with mGFP was determined by confocal microcopy in tumor and non-tumor areas of mTom-mGFP mice whose hepatocytes had been labeled via AAV8-TBG-Cre and that were subsequently treated with DEN and DDC diet (n=4). Scale bars 50 µm. ** p<0.01. Statistical significance was determined by two-sided T test.

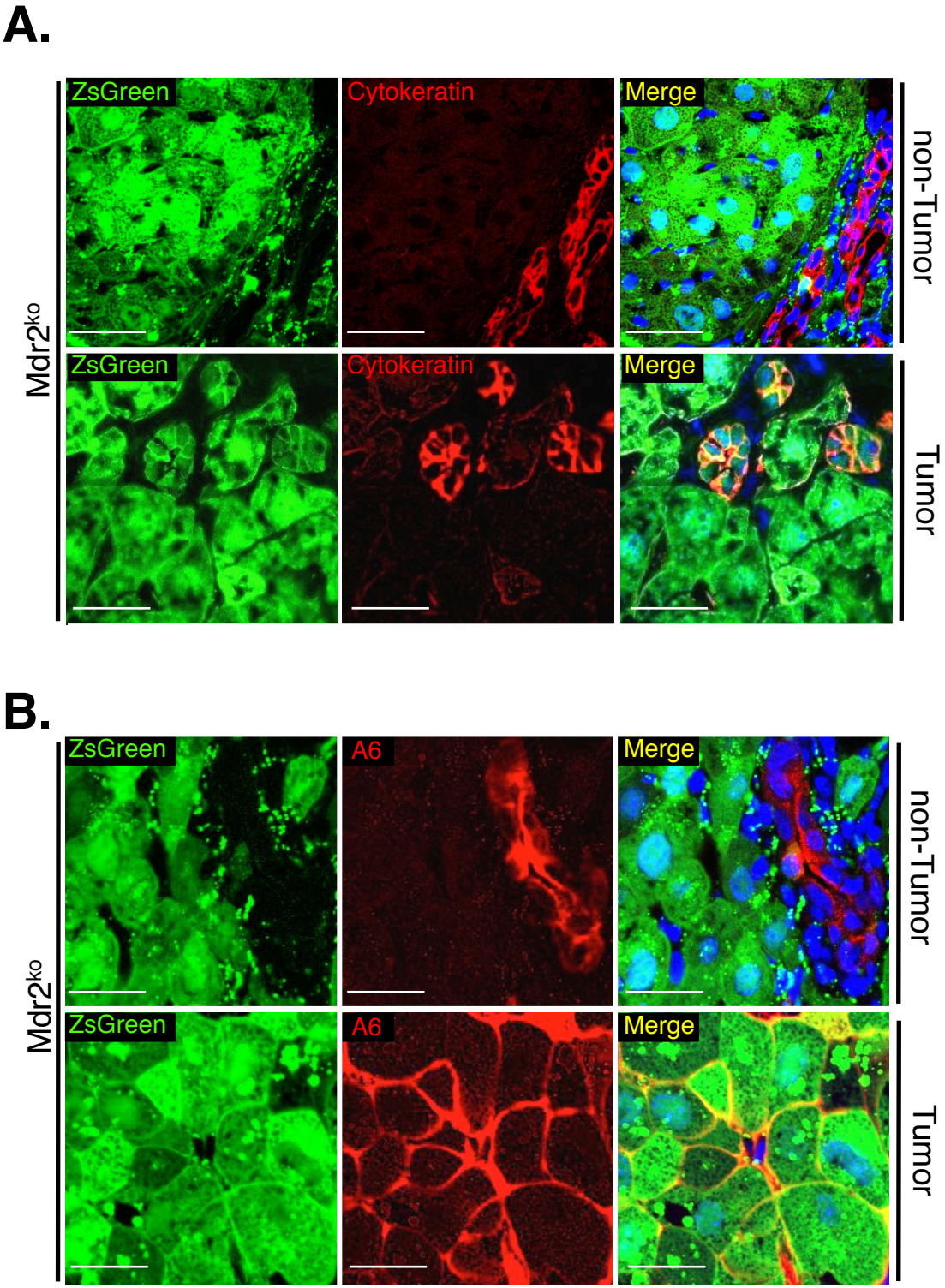

Supplementary Figure 15. Cytokeratin-positive liver progenitors within HCCs from Mdr2^{ko} mice are derived from hepatocytes. Colocalization of cytokeratin with ZsGreen was determined by confocal microcopy in tumor and non-tumor areas of Mdr2^{ko} mice expressing Cre reporter ZsGreen whose hepatocytes had been labeled via AAV8-TBG-Cre (n=7). Scale bars 50 µm.